Tropical Ocean-Atmosphere Interaction, the Pacific Cold Tongue, and the El Niño–Southern Oscillation

F.-F. Jin

The tropical Pacific basin allows strong feedbacks among the trade winds, equatorial zonal sea surface temperature contrast, and upper ocean heat content. Coupled atmosphere-ocean dynamics produce both the strong Pacific cold tongue climate state and the El Niño–Southern Oscillation phenomenon. A simple paradigm of the tropical climate system is presented, capturing the basic physics of these two important aspects of the tropic Pacific and basic features of the climate states of the Atlantic and Indian ocean basins.

Although solar heating is zonally uniform, the sea surface temperature (SST) in the tropics is far from zonally symmetric. In particular, the tropical Pacific features the largest zonal contrast in SST along the equator, with a warm pool in the west and a cold tongue in the east, and the strongest SST interannual fluctuations in the cold tongue region. This interannual variability is dominated by the well-known El Niño–Southern Oscillation (ENSO) phenomenon, which affects much of the global climate (*1*). Great progress has been made over the past decade in understanding and predicting ENSO (*2–7*) and in understanding the Pacific cold tongue (*8*). However, comprehending these two intimately related aspects of tropical climate system in one unified paradigm remains a challenge. In this report, a simple conceptual coupled model that reproduces the basic features of both aspects is presented.

Bjerknes (*9*) first hypothesized that a positive feedback of tropical ocean-atmosphere interaction can amplify SST perturbations of the cold tongue to sustain either a warm or a cold phase of ENSO. On one hand, the easterly trade winds force the thermocline depth, representing the layer of sharp vertical temperature gradient that separates the upper ocean from the abyssal deep ocean, to be shallower in the equatorial eastern Pacific than in the western Pacific. The trade winds also induce the equatorial Ekman upwelling because of Coriolis effects, which effectively brings the cold water from the subsurface to the surface layer to generate a cold tongue in the eastern Pacific. On the other hand, the atmospheric zonal pressure gradient caused by the east-west contrast of the SST drives an equatorial zonally asymmetric circulation (Walker circulation), which enhances the surface easterlies over the Pacific basin and thus strengthens the cold tongue.

Department of Meteorology, School of Ocean and Earth Science and Technology, University of Hawaii at Manoa, Honolulu, HI, USA.

Two decades later, the essential phase-transition mechanism of ENSO was added to this coupled positive-feedback hypothesis. It was found that during warm (cold) ENSO phases, the equatorial heat content is often draining out (building up) as a result of the mass exchange between the equatorial belt and off-equatorial regions by means of ocean dynamical adjustment (*2, 10*). This discharge and recharge of the equatorial heat content, which is out of phase with the SST anomalies of ENSO, was proposed (*2, 10*) as the cause of ENSO phase transitions. This recharge-oscillation mechanism is at the heart of ENSO theory, pointing to the instability of the tropical Pacific climate state, which supports a delayed oscillator (*11*), or more generally, a mixed SST-ocean dynamics mode (*7, 12*). While the ENSO research has been focusing on anomalies of the tropical coupled system, it has become clear that the positive feedback hypothesis of Bjerknes also offers an explanation for the zonal asymmetry in the mean (time-averaged) climate state of the tropical Pacific (*8*). Several decades of research, therefore, has brought us to the point where the two important aspects of tropical climate system, ENSO and the Pacific warm pool–cold tongue climate state, can be understood in a unified manner as first envisioned by Bjerknes (*9*).

A coupled two-box model was used to depict the positive feedback of the tropical ocean-atmosphere interaction and the ocean dynamic adjustment. The equatorial Pacific basin was divided into an eastern and a western half to distinguish the cold tongue and the warm pool. The temperature of the well-mixed surface layer of the eastern basin is then controlled by

$$\frac{dT_e}{dt} = -\varepsilon_T(T_e - T_r) - M(w)(T_e - T_{se})/H_m \tag{1}$$

where

$$M(w) = \begin{cases} 0, & w \le 0 \\ w, & w > 0 \end{cases}$$

The first term on the right side of Eq. 1 represents the net heating due to radiative, sensible, and latent heat fluxes through the ocean surface. This net heating is parameterized by a collective feedback parameter ε_T, which measures the rate at which the SST (T_e) is restored to a zonally uniform radiative-convective equilibrium temperature (T_r). The second term represents dynamical cooling due to the upwelling of the cold subsurface water (at temperature T_{se}) into the surface layer. Upwelling velocity is denoted by w, H_m is the mixed layer depth (about 50 meters), and the function $M(w)$ results from upstream vertical differencing. The poleward surface Ekman currents, which compensate for the equatorial upwelling, do not alter the equatorial SST, and relatively small zonal advection, which may have some impact on the western Pacific SST, is ignored (*13*). The SST in the western Pacific is assumed at radiative-convective equilibrium (T_r) as the first-order approximation, although the mechanisms that limit the warm pool temperature to about 30°C are subject to debate (*14*). Nevertheless, neglecting ocean dynamical cooling is consistent with the observation that there is little net heat flux through the warm-pool ocean surface (*15*) and that the atmosphere over the warm pool is nearly neutral (*16*) with adiabatic cooling from the ascending motion of Walker circulation largely balanced by latent heating.

The equatorial upwelling is largely attributable to Ekman pumping, which is mainly proportional to the zonal wind stress τ

$$w = -\alpha\tau = -\alpha[\tau_0 - \mu(T_r - T_e)] \tag{2}$$

where α depends on the latitudinal variation of the Coriolis parameter and the momentum mixing rate in the upper ocean [for example, α can be determined from equations A8 through A10 in (*3*)]. The equatorial zonal wind stress in Eq. 2 has two parts. The first part (τ_0) represents a zonally symmetric Hadley circulation resulting from the meridional differential heating of the atmosphere. The second part represents the Walker circulation, which ascends over the western Pacific warm pool and descends over the eastern Pacific cold tongue, driving an easterly surface wind over the equatorial Pacific. The approximate balance between the adiabatic warming as a result of the descending motion of the Walker circulation and the heat loss to the underlying cold surface implies that the intensity of the Walker circulation is closely related to the zonal contrast of atmospheric heating. The parameter μ is a feedback coefficient that measures the efficiency of the zonal differential heating in driving the Walker circulation.

The subsurface temperature depends strongly on the thermocline depth. By considering a typical vertical temperature profile of the tropical Pacific, it can be parameterized as (*17*)

$$T_{se} = T_r - (T_r - T_{r0}) \{1 - \tanh[(H + h_e - z_0)/h^*]\}/2 \qquad (3)$$

where T_{r0} is the temperature beneath the thermocline, h_e is the departure of thermocline depth in the eastern equatorial Pacific from its reference depth H, z_0 is the depth at which w takes its characteristic value, and h^* measures the sharpness of the thermocline.

The Sverdrup balance (*5*) between the pressure gradient force and wind stress over the equator constrains the east-west contrast of the thermocline depth

$$h_e = h_w + bL\tau \qquad (4)$$

where h_w denotes the departure of the thermocline depth in the western equatorial Pacific from the reference depth H and $bL\tau$ is proportional to the zonally integrated wind stress in the equatorial region: L is the ocean basin size, and b measures the efficiency of wind stress in driving the thermocline tilt. Thermocline depth h_w adjusts slowly to the zonally integrated Sverdrup meridional mass transport resulting from the wind-forced equatorial Rossby waves and follows

$$\frac{dh_w}{dt} = -rh_w + \frac{rbL\tau}{2} \qquad (5)$$

Parameter r measures the basin-wide dynamic adjustment rate; $rbL\tau/2$ represents the zonally integrated Sverdrup meridional mass transport, and the factor $r/2$ constrains the zonal mean thermocline depth at the equilibrium state to be the same as the reference depth. Conceptually, this equation simply describes the slow dynamic renewal of the warm pool heat content. It can also be derived from shallow-water dynamics with proper eastern and western boundary conditions for equatorial oceanic Kelvin and Rossby waves (*18*) and approximations for the filtering out of wave propagating processes.

Equations 1 to 5 form a simple coupled conceptual model for the tropical Pacific. Given an easterly surface wind driven by the Hadley circulation ($\tau_0 < 0$), the coupled system has a unique steady-state solution representing a strong cold tongue climate state at the eastern Pacific (Fig. 1). This equilibrium state is determined by the balance between the net heat flux into the

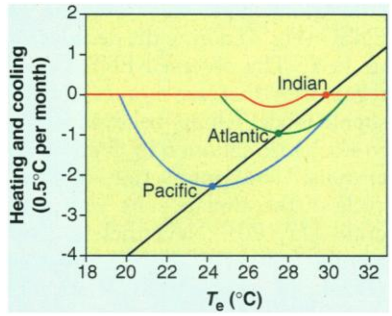

Fig. 1. Graphical solutions to the coupled model for the three tropical ocean basins. Net heating (reversed sign, black straight line for all the three basins) and dynamical cooling (colored curves) are plotted versus T_e under ocean dynamic equilibrium. Model climate states for the three ocean basins are indicated by the intersection points. The radiative-convective equilibrium temperature and warm pool temperature were set to T_r = 30°C. The other model parameters were chosen as ε_T = 1/(150 days), r = 1/(300 days), T_{r0} = 18°C, H = 100 m, z_0 = 75 m, h^* = 50 m, $\mu\alpha/H_m$ = (0.15/2)°C/month, μbL = 12.5 m/°C, and τ_0/μ = −1°C for the Pacific basin. For the Atlantic, μbL was reduced by half, and for the Indian Ocean, τ_0/μ was in addition changed to 1°C, whereas the other parameters for the Atlantic and Indian oceans were kept the same as those for the Pacific.

surface layer and the dynamical cooling of the SST as a result of the upwelling of the subsurface cold water. In the equilibrium state for the Pacific basin, the cold tongue temperature is about 24.5°C, and the net heating rate is about 2.3°C every 2 months, which is equivalent to a net surface heat flux of about 60 to 85 W/m^2 for a mixed layer depth of 35 to 50 m. Both of these values agree well with observations (*15*). The zonally asymmetric coupled dynamics are essential for cold tongue formation; without the coupled dynamics, the SST in the climate state is nearly zonally uniform. The intensity of the cold tongue is also sensitive to the SST restoration rate (ε_T). A moderate change in restoration rate (change in the slope of the black line in Fig. 1) can shift the cold tongue SST by a few degrees. The strong sensitivity of the Pacific cold tongue to the asymmetric coupled dynamics and the restoration rate is likely responsible for the scatter of the results in the simulations of tropical Pacific climate by coupled ocean-atmosphere general circulation models (*6*, *19*).

Basin size is also crucial to zonally asymmetric coupled dynamics. This becomes clear when the Atlantic is compared with the Pacific. The basin size L of the Atlantic is about one half that of the Pacific. With equally intense trade wind forcing, h_e in the eastern Atlantic is about one half that in the eastern Pacific because the east-west contrast of the thermocline depth depends on the integrated stress over the basin. The dynamical cooling, which is sensitive to h_e, is thus significantly weaker in the eastern Atlantic than it is in the Pacific. This effect brings the intensity of the Atlantic cold tongue down to about half of that of the Pacific (Fig. 1), although other factors not included in the model, such as the effects of land masses on atmospheric circulation, may also contribute to the differences of the cold tongue intensities of the two ocean basins.

The component of wind stress that is unrelated to the SST zonal contrast, τ_0, is another factor affecting the cold tongue. If

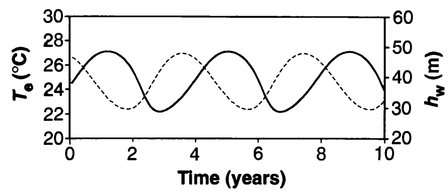

Fig. 2. Time series of (dashed curve) departure of the thermocline depth from the reference depth in the western Pacific and (solid curve) SST in the eastern Pacific.

$\tau_0 = 0$ (which represents the absence of the Hadley circulation), then the system has two equilibrium solutions: an unstable symmetric state and a weaker cold tongue state. Thus, the Hadley circulation suppresses the zonally uniform warm state and strengthens the cold tongue, although this condition is not essential for cold tongue formation in the Pacific Ocean. For the equatorial Indian Ocean, τ_0 can be positive as a result of the westerly wind of the Walker circulation associated with the western Pacific warm pool. The climate state of the Indian Ocean maintains a zonally uniform SST (Fig. 1) because of this small positive τ_0 as well as its small basin size, suggesting that asymmetric coupled dynamics play little role in the basic climate state of the Indian Ocean, the only basin without an equatorial cold tongue.

The equilibrium solutions of the coupled conceptual model (Fig. 1) describe the basic features of the tropical climate states of the three different ocean basins. Stability analyses by linearization of the model with respect to these steady states of the three basins indicate that climate states of the Indian and Atlantic oceans are stable, whereas the strong cold tongue state of the Pacific Ocean is unstable and bifurcates to an oscillatory solution. A typical oscillatory solution (Fig. 2) has a period of about 4 years. The deepening of the western thermocline depth leads the warm SST in the eastern Pacific by over a quarter of the cycle. This oscillatory solution for the Pacific basin agrees well with the observed ENSO (Fig. 3) during the decade from 1980 to 1990. The observed ENSO exhibits irregularities that are not captured by the simple model but are believed to be related to stochastic agitation by abundant "weather noise" and interaction of the annual cycle of the climate state with the ENSO cycle (*17, 20*). Nevertheless, the fundamental features of ENSO variability, the periodicity and the phase relation between the SST in the eastern Pacific and the thermocline depth or the sea level [highly related to heat content (*10*) of the western Pacific], are captured by the simple oscillation that arises from the unstable cold tongue state.

The instability and oscillation mechanisms of the ENSO associated with the Pacific cold tongue state can be highlighted by the linearized conceptual model

$$\frac{dh'_w}{dt} = -rh'_w - \frac{rbL\mu T'_e}{2}$$

$$\frac{dT'_e}{dt} = RT'_e + \gamma h'_w \qquad (6)$$

where

$$R = -\varepsilon_T \frac{\varepsilon}{1+\varepsilon} + \gamma bL\mu - \frac{M(\overline{w})}{H_m}$$

$$\varepsilon = -\frac{\tau_0}{\mu(T_r - \overline{T}_e)}$$

$$\gamma = \frac{M(\overline{w})}{H_m}\frac{\partial \overline{T}_{se}}{\partial \overline{h}_e} \qquad (7)$$

Overbar and prime in Eqs. 6 and 7 denote the steady state and derivations from the steady state, respectively, ε is the ratio between the Hadley and Walker circulation of the steady state, γ denotes the sensitivity of the subsurface temperature to the thermocline depth, and R collectively represents Bjerknes feedback processes for the SST growth. The frequency at a neutral growth rate ($R = r$) is $\sqrt{r\gamma bL\mu/2 - r^2}$, which depends heavily on $r\gamma bL\mu/2$, a term that combines the thermocline feedback (γ) and the recharge mechanism ($rbL\mu/2$). The Pacific cold tongue state is unstable when R is positive and overtakes the damping rate (r) in the ocean adjustment. The strong thermocline feedback is crucial for such an instability because Ekman pumping feedback alone is unable to overcome the restoration damping. If a cold tongue is too strong or too weak, this thermocline feedback will be reduced, and ENSO-like oscillations cannot be sustained. Thus, the weak Atlantic cold tongue has no vigorous ENSO-like interannual variability (*21*). The unstable mode of the system in Eq. 6 is the maximum simplification to the mixed SST–ocean dynamics mode captured by a more complicated framework for the tropical interannual variability (*12*). The out-of-phase relation between an SST anomaly of the eastern Pacific and a thermocline depth anomaly of the western Pacific results from the recharge and discharge of the equatorial heat content associated with slow ocean dynamic adjustment, which is fundamental to the cyclic behavior of the ENSO.

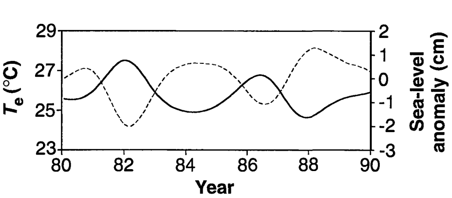

Fig. 3. Time series of (dashed curve) the observed sea-level anomaly over the western Pacific averaged from 10°N to 10°S and from 120°E to the dateline and (solid curve) SST averaged from 5°N to 5°S and from 90°W to 150°W for the years 1980 to 1990. A 13-month running mean was applied twice to the monthly data after the mean annual cycle was removed. The sea-level data are from the University of Hawaii Sea-Level Center, and the SST data from the Comprehensive Ocean-Atmosphere Data Set (COADS) of the National Center of Atmospheric Research.

An ENSO cycle can be illustrated by starting with, for instance, an initial positive SST anomaly in the eastern Pacific. This initial SST anomaly induces an anomalous equatorial westerly wind, which reduces the upwelling and deepens the thermocline in the eastern Pacific, thus leading to less dynamical cooling. The warm SST anomaly also results in less net heating. When the reduction in dynamical cooling is more than the loss of heating, the initially warm SST anomaly is further amplified. Such a positive feedback process brings the system to a mature warm ENSO phase bounded by nonlinearity. At the same time, the thermocline depth in the western Pacific and the zonal mean thermocline depth gradually adjust to the westerly wind anomaly by the anomalous discharge of the heat content in the equatorial ocean into off-equatorial regions. In the aftermath of the warm event, the zonal mean thermocline depth becomes shallower across the Pacific, while the equatorial ocean takes time to refill. This anomalous shallow zonal mean thermocline depth at the transition allows anomalously colder water to be pumped into the surface layer and leads the SST anomaly to a cold phase, which is then similarly amplified through the coupled positive-feedback process. The recharging of equatorial heat content during the cold phase with anomalously strong trade winds leads to an anomalously deep zonal mean thermocline depth. By the time the cold event diminishes, the deep zonal mean thermocline initiates the next warm phase.

This conceptual model of the tropical ocean-atmosphere system provides a paradigm that unifies our understanding of both the ENSO and the climate states of the equatorial ocean basins. Other aspects of the tropical climate—such as north-south asymmetry and monsoon circulation, which involve feedback between the Hadley circulation and meridional SST gradient and atmosphere-ocean-land interactions—are not captured in this model. Our understanding of the climate state of the global tropics and its variability will be enriched as a more comprehensive paradigm comprising all of these fundamental aspects of the tropical climate emerges.

REFERENCES AND NOTES

1. E. M. Rasmusson and T. H. Carpenter, *Mon. Weather Rev.* **110**, 354 (1982); M. A. Cane, *Science* **222**, 1189 (1983); E. M. Rasmusson and J. M. Wallace, *ibid.*, p. 1195; S. G. H. Philander, *Nature* **302**, 295 (1983).
2. M. A. Cane and S. E. Zebiak, *Science* **228**, 1085 (1985); M. Cane, S. E. Zebiak, S. C. Dolan, *Nature* **321**, 827 (1986).
3. S. E. Zebiak and M. Cane, *Mon. Weather Rev.* **115**, 2262 (1987).
4. T. Barnett *et al.*, *Science* **241**, 192 (1988).
5. S. G. H. Philander, *El Niño, La Niña, and the Southern Oscillation* (Academic Press, San Diego, CA, 1990).
6. J. D. Neelin *et al.*, *Clim. Dyn.* **7**, 73 (1992).
7. J. D. Neelin, M. Latif, F.-F. Jin, *Annu. Rev. Fluid Mech.* **26**, 617 (1994).
8. H. A. Dijkstra and J. D. Neelin, *J. Clim.* **8**, 1343 (1995).
9. J. Bjerknes, *Mon. Weather. Rev.* **97**, 163 (1969).
10. K. Wyrtki, *J. Geophys. Res.* **91**, 7129 (1986).
11. P. S. Schopf and M. J. Suarez, *J. Atmos. Sci.* **45**, 549 (1988); D. S. Battisti and A. C. Hirst, *ibid.* **46**, 1687 (1989).
12. F.-F. Jin and J. D. Neelin, *J. Atmos. Sci.* **50**, 3477 (1993), J. D. Neelin and F.-F. Jin, *ibid.*, p. 3504; F.-F. Jin and Neelin, *ibid.*, p. 3523.
13. A separate calculation has shown that inclusion of the horizontal advection modifies the results only quantitatively.
14. V. Ramanathan and W. Collines, *Nature* **351**, 27 (1991); R. Fu, A. D. Del Genio, W. B. Rossow, W. T. Liu, *ibid.* **358**, 394 (1992); J. M. Wallace, *ibid.* **357**, 230 (1992); D.-Z. Sun and Z. Liu, *Science* **272,** 1148 (1996).
15. S. K. Esbensen and Y. Kushnir, *Clim. Res. Inst. Rep. No. 29* (Department of Atmospheric Science, Oregon State University, Corvallis, 1981).
16. K. A. Emanuel, J. D. Neelin, C. S. Bretherton, *Q. J. R. Meteorol. Soc.* **120**, 1111 (1994).
17. F.-F. Jin, J. D. Neelin, M. Ghil, *Physica D*, in press.
18. M. Cane and E. S. Sarachik, *J. Mar. Res.* **39**, 651 (1981).
19. C. R. Mechoso *et al.*, *Mon. Weather Rev.* **123**, 2825 (1995).
20. F.-F. Jin, J. D. Neelin, M. Ghil, *Science* **264**, 70 (1994); E. Tziperman, L. Stone, M. A. Cane, H. Jarosh, *ibid.*, p. 72; P. Chang, B. Wang, T. Li, J. Lin, *J. Atmos. Sci.* **52**, 2353 (1995).
21. S. E. Zebiak, *J. Clim.* **6**, 1567 (1993).

22. This work was supported by NSF grant ATM-9312888 and NOAA grant GC95773. I thank D. Neelin, T. Schroeder, and anonymous reviewers for valuable comments that improved the manuscript, D. Henderson for her careful reading of the manuscript, and the University of Hawaii Sea Level Center for providing the sea-level data. School of Ocean and Earth Science and Technology contribution 4134.

3 June 1996; accepted 20 August 1996